Journal of Aerosol Science 101 (2016) 10–21

Contents lists available at ScienceDirect

Journal of Aerosol Science

journal homepage: www.elsevier.com/locate/jaerosci

Predictions on dynamic evolution of compositional mixing degree in two-component aggregation

Hanqing Zhao, Zuwei Xu*, Haibo Zhao*

State Key Laboratory of Coal Combustion, School of Energy and Power Engineering, Huazhong University of Science and Technology, Wuhan 430074, PR China

ARTICLE INFO

Article history:
Received 3 January 2016
Received in revised form
27 April 2016
Accepted 5 July 2016
Available online 14 July 2016

Keywords:
Population balance modeling
Two-component aggregation
Compositional mixing degree
Particle size distribution

ABSTRACT

The compositional distribution in two-component aggregative mixing of initially bidisperse particle populations can be described by a Guassian-type function, which is determined by the mixing degree χ (assessed quantitatively by the mass-normalized power density of excess component A), and the overall mass fraction ϕ (a known value from the initial feeding condition) of component A. It is known that χ will reach a steady-state value χ_∞ over time (factually, after attaining the self-preserving size distribution), and χ_∞ is only relevant to ϕ, namely the feeding condition. However, the dynamic evolution of χ before the attainment of a steady-state value is not exactly known. In this paper, the fast differentially-weighted Monte Carlo method for population balance modeling was used to predict the dependence of time-varied χ on initial feeding conditions through hundreds of systematically varied simulations. It is found that χ is subject to an exponential decay, largely depending on the ratio of steady-state mixing degree and its initial value (χ_∞/χ_0). With the explored exponential formulas for the dynamic mixing degree, it is possible to attain an optimum control on the compositional distributions during two-component aggregation processes through selecting the initial feeding parameters, and the time needed for reaching a steady-state is investigated.

1. Introduction

In the research of particle behavior, multicomponent aggregation has become a focal point, since it represents the basic physical mechanism of size enlargement (Hosseini, Bouaswaig, & Engell, 2013), and has a wide application in wet granulation (Barrasso & Ramachandran, 2012), crystallization (Hofmann & Raisch, 2013), atmospheric aerosols (Kuang, McMurry, & McCormick, 2009), granulation of powders (Iveson, 2002) and synthesis of nanoparticles (Friedlander & Smoke, 2000) etc. Nevertheless mostly studies focused on single component systems, theoretical analysis of two-component aggregation is just beginning. In order to study different particles properties during these processes, the evolution of the degree of mixing is of vital importance. Matsoukas, Lee, and Kim (2006) firstly studied the sum-square of excess component to quantify the degree of blending and certified it was constant under partially mixed states and kernels of the sum type. Then Lee, Kim, Rajniak, and Matsoukas (2008) defined a related intensive parameters χ (mixing degree) through normalizing the sum-square of excess component by the mass of all granules, which was proposed as the mass-normalized power density of

* Corresponding authors.
E-mail addresses: xuzw@hust.edu.cn (Z. Xu), klinsmannzhb@163.com (H. Zhao).

http://dx.doi.org/10.1016/j.jaerosci.2016.07.003
0021-8502/

excess component. Furthermore, the relationship between χ and mean particle size can test how the kernel influences blending of components (Matsoukas, Kim, & Lee, 2009) and the precision of computation method (Lee et al., 2008). χ is defined as (Marshall, Rajniak, & Matsoukas, 2011):

$$\chi = \frac{X^2}{M} = \frac{\int_0^\infty \mathrm{d}m \int_0^m \mathrm{d}m_\mathrm{A} x^2 f(m,t) g(m_\mathrm{A}|m,t)}{\int_0^\infty \mathrm{d}m \int_0^m \mathrm{d}m_\mathrm{A} m f(m,t) g(m_\mathrm{A}|m,t)} \tag{1}$$

where x is the amount of component A in excess of the amount ϕm: $x = m_\mathrm{A} - \phi m = m_\mathrm{A} - \phi(m_\mathrm{A} + m_\mathrm{B})$; X^2 is the sum-square of excess component; ϕ is the overall mass fraction of component A, keeping constant during aggregation: $\phi = N_{\mathrm{A}0} m_{\mathrm{A}0}/(N_{\mathrm{A}0} m_{\mathrm{A}0} + N_{\mathrm{B}0} m_{\mathrm{B}0})$; $f(m,t)$ is the component-independent particle size distribution function so that $f(m,t)\mathrm{d}m$ represents the number concentration of particles in the mass range of m to $m+\mathrm{d}m$; $g(m_\mathrm{A}|m)$ is the compositional distribution of component A, which is the fraction of particles of mass m that contain component A in the mass amount $(m_\mathrm{A}, m_\mathrm{A}+\mathrm{d}m_\mathrm{A})$.

Matsoukas et al. (2006) stressed the steady-state value of χ was the single most important parameter that decided the width of the distribution of components in all size classes and this value largely depended on the initial state, based on kernels that are independent of composition. This probability density $g(m_A|m)$ was certified as a Gaussian-type function theoretically in the steady state condition, then this conclusion was extended to the evolution process which could be expressed as (Lee et al., 2008; Zhao & Kruis, 2014):

$$g(m_\mathrm{A}|m,t) = \frac{1}{\sqrt{2\pi m \chi}} \exp\left[-\frac{(m_\mathrm{A} - \phi m)^2}{2m\chi}\right] \tag{2}$$

Depending on both composition-independent and -dependent kernels, it is found that the compositional distributions become self-preserving, when the degree of mixing (χ) reaches its steady-state value (Krapivsky & Ben-Naim, 1996; Vigil & Ziff, 1998). And this Gaussian-type form was validated through PBM based on the constant-number method and the differentially-weighted Monte Carlo method (Lee et al., 2008; Zhao, Kruis & Zheng, 2011). According to analysis and model fitting from hundreds of simulations, the steady-state value of χ (χ_∞) was well predicted by the initial feeding condition for Brownian aggregation either in the free-molecular (Zhao & Kruis, 2014):

$$\frac{\chi_\infty}{\chi_0} = \exp\left[-2(\phi - \phi_{\beta=1})^2\right] \tag{3}$$

or in the continuum regime:

$$\frac{\chi_\infty}{\chi_0} = \exp\left[-(\phi - \phi_{\beta=1})^2/\sqrt{2}\right] \tag{4}$$

where $\phi_{\beta=1}$ is a simplified expression of ϕ, when particle diameter ratio β is set as 1: $\phi_{\beta=1} = \frac{\alpha\gamma}{1+\alpha\gamma}$. α is the number ratio; γ is the density ratio between two components.

As there exists a prediction formula of χ_∞, we assume that there is a certain functional relation between $\chi(t)$ and the initial state parameters. This paper concentrates on investigating the whole evolution of the mixing degree based on reliable population balance modeling. First, based on Eq. (2), with known $\chi(t)$, the compositional distribution of each component can be obtained through the probability density function $g(m_\mathrm{A}|m)\mathrm{d}m_\mathrm{A}$. In this way, it is possible to predict and control the whole evolution of the compositional distribution and the degree of mixing to optimize two-component aggregative mixing by properly selecting the initial mass and number concentrations of component A and B in the feeding. Second, as an ultimate state, the steady-state is only approached by the previous investigators through waiting a long time (Matsoukas et al., 2009; Zhao & Kruis, 2014). The time needed (time-lag) to reach the steady-state can be obtained here.

For example, about gas-fluidization of nano-particle mixtures in magnetically assisted fluidized bed, the mixing degree and the compositional distributions of SiO_2 and ZnO can affect the fluidization stability (Zeng, Zhou & Yang, 2008). Thus if we know how the initial condition affects the mixing degree, it is able to optimize the fluidization performance in the whole process. Meanwhile this discussion can contribute to the mechanism explanation between the component distribution and the fluidization behavior. The dynamic evolution of the mixing degree is helpful for the optimal control of this kind process. From another point of view, during the Fe–Pt synthesis, we can know how long it takes to reach the steady-state or a certain composition distribution. Because Fe–Pt alloys with different Fe/Pt compositions have various crystal structures, chemical and physical properties, leading to different nominal atomic rations. It is helpful for investigating the way of crystal growth and the formation of different nominal atomic rations (Liu et al., 2014).

The aim of this paper is to gain insight into the functional relation between $\chi(t)$ and the certain parameters in the initial state of two-component aggregation processes, such as χ_0 (here $\chi_0 = (1-\phi)\phi(m_{\mathrm{A}0}(1-\phi) + m_{\mathrm{B}0}\phi)$), and the steady-state value χ_∞. The paper is organized as follows: first, in Section 2, to simulate two-component PBM we introduce the differentially weighted Monte Carlo (DWMC) method. Then in Section 3, the numerical results for Brownian aggregation are shown. By a series of initial conditions, the possible influencing factors on $\chi(t)/\chi_0$ are analyzed and an empirical formula giving an estimation of $\chi(t)/\chi_0$ is found. Finally, the empirical formula is validated and conclusions are given.

2. Methodology

Here the population balance-Monte Carlo (PBMC) method is adopted, which are capable of simulating a large number of internal variables in a straightforward manner. As the governing PBE, the Smoluchowski's equation for two-component aggregation is (Lushnikov, 1976):

$$\frac{\partial n(m_A,m_B,t)}{\partial t}=\frac{1}{2}\int_0^{m_A}\int_0^{m_B}K(m_A-m'_A,m_B-m'_B;m'_A,m'_B)n(m_A-m'_A,m_B-m'_B,t)n(m'_A,m'_B,t)\mathrm{d}m'_A\mathrm{d}m'_B - n(m_A,m_B,t)\int_0^{\infty}\int_0^{\infty}K(m_A,m_B;m'_A,m'_B,t)n(m'_A,m'_B,t)\mathrm{d}m'_A\mathrm{d}m'_B \quad (5)$$

Here $K(m_A,m_B;m'_A,m'_B)$ is the aggregation rate coefficient (kernel) between a particle (m_A,m_B) and another particle (m'_A, m'_B).

The differentially-weighted Monte Carlo method (DWMC) method is adopted here to determine the distributions of the multivariate properties over their full-spectrum more accurately, whereas conventional MC methods are accurate only in those regions of the spectra with sufficient simulation particles (Zhao, Kruis, & Zheng, 2010, 2011; Zhao & Zheng, 2011, 2013). The weight of a differentially weighted particle i, w_i, indicates that the simulation particle i represents w_i real particles having the same internal variables as i.

In the transition regime A, the kernel is composed by Brownian coagulation kernel in the slip flow regime K_{ij}^{sf}, and Brownian coagulation kernel in the free molecular regime K_{ij}^{fm}, where $K_{ij}^{\mathrm{sf}}=K_{\mathrm{co}}\left(v_i^{1/3}+v_j^{1/3}\right)\left[\frac{C_i}{v_i^{1/3}}+\frac{C_j}{v_j^{1/3}}\right]$, ${}^{sf}\hat{K}_{ij}^{'}=2K_{\infty}w_jC_j\left[1+\frac{C_{\max}}{C_j}+\left(\frac{v_{\max}}{v_j}\right)^{1/3}+\frac{C_{\max}}{C_j}\left(\frac{v_j}{v_{\min}}\right)^{1/3}\right]$; the slip correction factor $C_j=1+2.514\lambda\left(\frac{6v_j}{\pi}\right)^{-1/3}$,$C_{\max}=1+2.514\lambda\left(\frac{6v_{\min}}{\pi}\right)^{-1/3}$; λ is the mean free path of the medium (Kazakov & Frenklach, 1998; Patterson, Singh, Balthasar, Kraft, & Wagner, 2006).

However in the Brownian coagulation in the transition regime B, we adopt the physically realistic Brownian collision kernel (Jacobson, 2005); for normal kernel, the Stokes-Cunningham slip correction factor is redefined as $C_i=1+\frac{\lambda}{d_i}\left[2.493+0.84\exp(-0.435d_i/\lambda)\right]$; the diffusion coefficient for particle i is $D_i=\frac{k_BT}{3\pi\mu d_i}\left[\frac{5+4Kn_i+6Kn_i^2+18Kn_i^3}{5-Kn_i+(8+\pi)Kn_i^2}\right]$; the velocity of particle i is $\bar{c}_i=\left(\frac{8k_BT}{\pi m_i}\right)^{1/2}$; the transition parameter of particle i is $g_i=\frac{1}{3d_il_i}\left[(d_i+l_i)^3-\left(d_i^2+l_i^2\right)^{\frac{3}{2}}\right]-d_i$; for majorant kernel, two simplified kernel is $\widehat{K}'_i(d_i,d_j)=C_a\left[d_i+d_j+C_b\left(d_i^{1/2}+d_j^{1/2}+\frac{C_c}{d_i^{1/2}}+\frac{C_c}{d_j^{1/2}}\right)\right]\left(d_i^{-1}+d_j^{-1}+C_cd_i^{-2}+C_cd_j^{-2}\right)$ and $\widehat{K}'_2(d_i,d_j)=K_{\mathrm{fm}}(d_i+d_j)^2(d_i^{-3/2}+d_j^{-3/2})$ respectively, where $C_a=\frac{2k_BT}{3\mu}$, $C_b=\frac{\sqrt{16k_BT\rho_P/27}}{\pi\mu}$, $C_c=3.39\lambda$.

Then the fast DWMC method is used to accelerate PBMC simulation (Xu, Zhao, & Zheng, 2014, 2015), where the majorant of coagulation kernel $\hat{K}_{ij}$ is developed to calculate the coagulation probability of all particle pairs by single looping over all particles rather than double looping. We consider six kinds of kernel, especially for Brownian kernel in the transition regime, which is added here by two different kernels A and B. One is simplified; the other is more complex and realistic (Wei, 2014).

Table 1 summarizes six typical aggregation kernels in different regimes and their weighted majorant kernels, and Table 2 shows the specific conditions in simulation cases.

3. Results

3.1. $\chi(t)/\chi_0$ for Constant coagulation and Linear coagulation

The fast DWMC is used to simulate 25 valid cases (Case 5, 6 in Table 2) of more simplified kernel Constant coagulation and Linear coagulation, respectively. It has been concluded that if the kernel can be expressed in additive contributions from granule, i.e.:

$$K(m_A,m_B;m'_A,m'_B)=K(m_A,m_B)+K(m'_A,m'_B) \quad (6)$$

Leading (Matsoukas et al., 2009)

$$\mathrm{d}\chi/\mathrm{d}t=0 \quad (7)$$

In this case, the variance of excess solute is constant during aggregation and equal to its value at zero, regardless of initial conditions. The simulation results certify the conclusion, that all the cases with varied α, β leading to the same constant evolution for Linear coagulation. Here time is made dimensionless with the characteristic aggregation time scale, τ_{coag}, which is defined as $1/(2\overline{K}_0N_0)$ for an initially bidisperse distribution, and $\overline{K}_0$ is the initial mean kernel over all possible particle pairs. However for more usual cases like Brownian coagulation, Eq. (7) is not satisfied any more, which is emphasized in this paper.

Table 1
Normal kernels and weighted majorant kernels.*

Case		Formulation
Constant coagulation	Normal kernel	$K_{ij}=\mathrm{A}$
	Weighted majorant kernel	$\hat{K}_{ij}^{'}=2\mathrm{A}w_j$
Linear coagulation	Normal kernel	$K_{ij}=\mathrm{A}(v_i+v_j)$
	Weighted majorant kernel	$\hat{K}_{ij}^{'}=2\mathrm{A}w_j v_j\left(1+\frac{v_{\max}}{v_j}\right)$
Brownian coagulation in the free molecular regime	Normal kernel	$K_{ij}=K_{\mathrm{fm}}(v_i^{1/3}+v_j^{1/3})^2(v_i^{-1}+v_j^{-1})^{1/2}$
	Weighted majorant kernel	$\hat{K}_{ij}^{'}=2\sqrt{2}K_{\mathrm{fm}}v_j^{1/6}w_j\left[\left(\frac{v_{\max}}{v_j}\right)^{2/3}+\left(\frac{v_{\max}}{v_j}\right)^{1/6}+1+\left(\frac{v_{\min}}{v_j}\right)^{-1/2}\right]$
Brownian coagulation in the continuum regime	Normal kernel	$K_{ij}=K_{\mathrm{co}}(v_i^{1/3}+v_j^{1/3})(v_i^{-1/3}+v_j^{-1/3})$
	Weighted majorant kernel	$\hat{K}_{ij}^{'}=2K_{\mathrm{co}}w_j\left[2+\left(\frac{v_{\max}}{v_j}\right)^{1/3}+\left(\frac{v_{\min}}{v_j}\right)^{-1/3}\right]$
Brownian coagulation in the transition regime A	Normal kernel	$K_{ij}=\left(\frac{1}{K_{ij}^{sf}}+\frac{1}{K_{ij}^{fm}}\right)^{-1}$
	Weighted majorant kernel	$\hat{K}_{ij}^{'}=\left(\frac{1}{{}^{sf}\hat{K}_{ij}^{'}}+\frac{1}{{}^{fm}\hat{K}}^{'}\right)^{-1}$
Brownian coagulation in the transition regime B	Normal kernel	$K_{ij}=2\pi(d_i+d_j)(D_i+D_j)\left(\frac{d_i+d_j}{d_i+d_j+(g_i^2+g_j^2)^{\frac{1}{2}}}+\frac{8(D_i+D_j)}{(d_i+d_j)+(\bar{c}_i^2+\bar{c}_j^2)^{\frac{1}{2}}}\right)^{-1}$
	Weighted majorant kernel	$\hat{K}_{ij}^{'}=2w_{\max}\ \min\ (\hat{K}_1^{'}+\hat{K}_2^{'})^{-1}$

* A is a constant number; $K_{\mathrm{fm}}=\left(\frac{3}{4\pi}\right)^{1/6}\left(\frac{6k_{\mathrm{B}}T}{\rho_{\mathrm{p}}}\right)^{1/2}$, $K_{\mathrm{co}}=\frac{2k_{\mathrm{B}}T}{3\mu}$; k_{B} is Boltzmann's constant; T is the thermodynamics temperature of the medium; ρ_{p} is the density of the particles; and μ is the viscosity of the medium.

Table 2
Conditions used in simulation cases: the volume of the computational domain, the number concentration ratio α and particle diameter ratio β are varied in the simulations.

	N_{A0} (m^{-3})	d_{A0} (μm)	ρ_{A0} ($\mathrm{kg\ m}^{-3}$)	ρ_{B0} ($\mathrm{kg\ m}^{-3}$)	T (K)	μ (Pa s)
Case 1, Brownian coagulation in the free molecular regime	9×10^{21}	0.001	21.45×10^3	21.45×10^3	1800	5.65×10^{-5}
Case 2, Brownian coagulation in free-molecular regime	9×10^{21}	0.001	7.87×10^3	21.45×10^3	1800	5.65×10^{-5}
Case 3, Brownian coagulation in continuum regime	3×10^{15}	0.5	2.00×10^3	2.00×10^3	300	1.81×10^{-5}
Case 4, Brownian coagulation in transition regime A and B;	4×10^{21}	0.002	7.87×10^3	7.87×10^3	1800	5.65×10^{-5}
Case 5, Constant coagulation	4×10^{21}	0.002	7.87×10^3	7.87×10^3	1800	5.65×10^{-5}
Case 6, Linear coagulation	4×10^{21}	0.002	7.87×10^3	7.87×10^3	1800	5.65×10^{-5}

3.2. Screening the relevant parameters for $\chi(t)/\chi_0$ in Brownian coagulation

During the whole evolution process, the value of $\chi(t)/\chi_0$ usually keeps the same order from its initial value to its steady one. Moreover, the steady value $\chi(t)/\chi_0$ is able to be well predicted by initial feeding condition and parameters associated with the Brownian aggregation kernel. So it is speculated that $\chi(t)/\chi_0$ is largely controlled by the initial degree of mixing. Introducing the following ratios:

$$\alpha=\frac{N_{\mathrm{A0}}}{N_{\mathrm{B0}}},\beta=\frac{d_{\mathrm{A0}}}{d_{\mathrm{B0}}},\gamma=\frac{\rho_{\mathrm{A}}}{\rho_{\mathrm{B}}} \tag{8}$$

Define the overall number fraction of component A:

$$\psi=\frac{N_{\mathrm{A0}}}{N_{\mathrm{A0}}+N_{\mathrm{B0}}}=\frac{\alpha}{1+\alpha} \tag{9}$$

and calculate the overall mass fraction of component A:

$$\phi=\frac{M_{\mathrm{A0}}}{M_{\mathrm{A0}}+M_{\mathrm{B0}}}=\frac{\alpha\beta^3\gamma}{1+\alpha\beta^3\gamma} \tag{10}$$

It is possible to calculate the initial degree of mixing χ_0 in the bidisperse case as (Lee et al., 2008; Matsoukas et al., 2009):

$$\chi_0 = (1-\phi)\phi(m_{A0}(1-\phi)+m_{B0}\phi) = \frac{\alpha\beta^3\gamma(1+\alpha)}{\left(1+\alpha\beta^3\gamma\right)^3}m_{A0} = \frac{\phi(1-\phi)^2}{(1-\psi)}m_{A0} \tag{11}$$

We concentrate on a large amount of simulation data, which is applied by the composition-dependent case (Case 2). Taking α at 10 as an example with varied β, Fig. 1 shows the mass-normalized power density of excess component A (χ) against time made dimensionless with the characteristic aggregation time scale, τ_{coag}. It is discovered that the evolution of $\chi(t)/\chi_0$ is monotone decreasing, and its decreasing rate slows down gradually. With time goes on, it approaches steady-state value. Among kinds of elementary functions, we deduce if it can be fitted with an exponential decay, in the formation:

$$\chi(t)/\chi_0 = \chi_\infty/\chi_0 + C_1\exp(-t/C_2) \tag{12}$$

where $\chi(t)/\chi_0$ decreases at a rate proportional to its current value:

$$\mathrm{d}\frac{\chi(t)}{\chi_0}\Big/\mathrm{d}t \propto -\frac{1}{C_2}\frac{\chi(t)}{\chi_0} \tag{13}$$

Here C_2 is called exponential time constant, as a relevant parameter of the rate. Meanwhile Eq. (13) satisfies the Markov model in the DWMC method, where future states depend only on the present state and not on the sequence of events that preceded it.

As shown in Fig. 2, more precisely at logarithmic axis, where MC simulation is repeated five times, and the standard error of Eq. (12) fitting is 6.325×10^{-4}. In addition, we can see the exponential law is fairly coincident with the simulation value during the evolution process, even if the steady-state value is not pretty stable. As long as the dimensionless steady-state

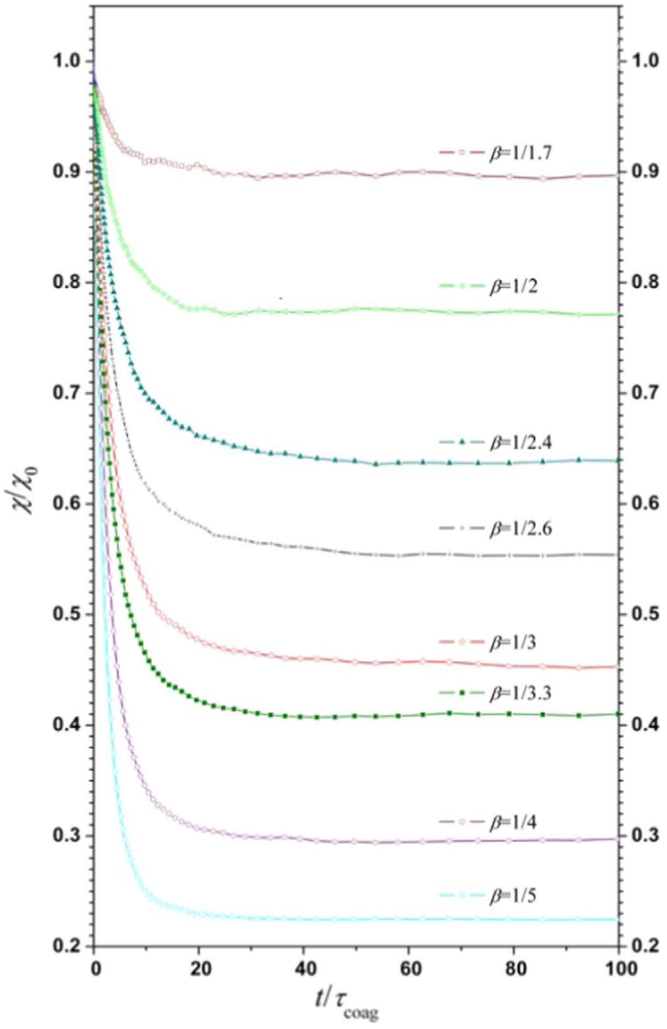

Fig. 1. $\chi(t)/\chi_0$ against the dimensionless time with α fixed at 10, varied β (Case 2).

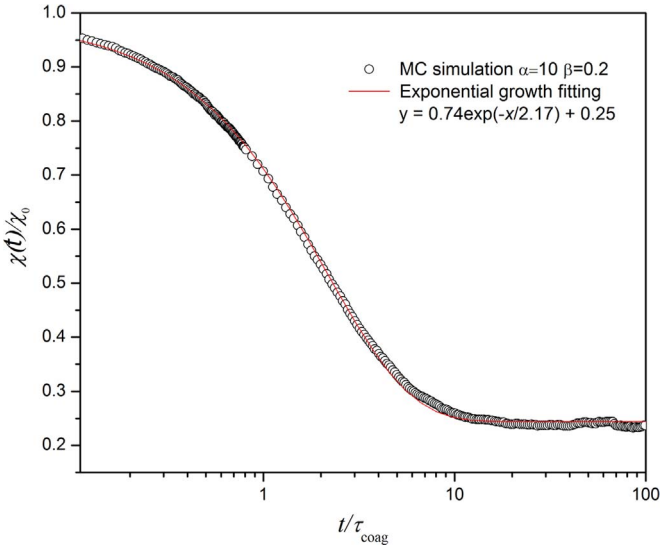

Fig. 2. $\chi(t)/\chi_0$ as function of the dimensionless time: satisfying exponential function (Case 1).

value is below 0.9, when there is a considerable decrease, the exponential formulation is able to describe the evolution process.

We introduce four coefficients altogether: C_1, C_2, C_3, C_4, to calculate the coefficients in the fitting function step by step, where $C_2=f(C_3, C_4)$. Firstly, it is evident from Eq. (12) at the beginning of the evolution

$$C_1+\chi_\infty/\chi_0=1 \tag{14}$$

At $t=0$, $\chi(0)/\chi_0$ is equal to 1. As shown in Fig. 3, MC simulation result agrees well with Eq. (14).

Then, we focus on C_2, which is a key parameter determining the evolution rate. Based on population balance modeling, the evolution of mixing degree is calculated as (Lee et al., 2008)

$$\frac{\mathrm{d}\chi}{\mathrm{d}t}=\frac{1}{M}\int_0^\infty \mathrm{d}m\int_0^\infty \mathrm{d}m'\int_0^m \mathrm{d}m_\mathrm{A}\int_0^{m'} \mathrm{d}m'_\mathrm{A}xx'\times K\left(m_\mathrm{A},m_\mathrm{B};m'_\mathrm{A},m'_\mathrm{B}\right) \times f(m,t)g(m_\mathrm{A}|m,t)f(m',t)g\left(m'_\mathrm{A}|m',t\right) \tag{15}$$

where $K(m_\mathrm{A},m_\mathrm{B};m'_\mathrm{A},m'_\mathrm{B})$ is the aggregation rate coefficient (kernel) between a particle (m_A,m_B) and another particle (m'_A, m'_B). Thus all the possible influence factors should be the contained in the Brownian aggregation kernel, which is detailed written in Table 1. Therefore $\chi(t)/\chi_0$ may be related to the following similar parameters: T, N_{A0}, d_{A0}, ρ_A, α, β, and γ.

For this analysis, it is certified that using different T while keeping the other parameters constant, does not influence $\chi(t)/\chi_0$ as well as χ/χ_0. Similarly, it is found that N_{A0}, d_{A0}, and ρ_A are non-influencing parameters for both χ_∞/χ_0 and $\chi(t)/\chi_0$ as long as the parameters α, β, and γ are kept constant (Zhao & Kruis, 2014). The independence of the time evolution of the degree of mixing from the values of T, N_{A0}, d_{A0}, and ρ_A is due to the dimensionless representation of the results and the dimensionless time τ_{coag}.

Obviously, the left three parameters α, β, and γ is thus concluded to be the parameters of the function $\chi(t)/\chi_0$.

The steady-state χ_∞/χ_0 and the evolution $\chi(t)/\chi_0$ depend on same parameters α, β, and γ. χ_∞/χ_0 has already been established by a combination of them as Eqs. (3) and (4) shown. We want to know if there exists a one-to-one correspondence between $\chi(t)/\chi_0$ and χ_∞/χ_0. However with a constant χ_∞/χ_0, there can be an evidently different evolution process as Fig. 4 show. To further explore their relation, the control variable method is adopted here. Once two parameters, for example α and γ are fixed, a deterministic relation between χ_∞/χ_0 and the remaining parameter β can be obtained by fitting the PBMC simulation results. Certainly, as an important indirect parameter χ_∞/χ_0, which is predicted by Eq. (3) in free molecular regime, it should be taken into account to help find regulations between $\chi(t)/\chi_0$ and α, β, γ.

3.3. $\chi(t)/\chi_0$ as function of α and β: composition-independent case ($\gamma=1$) in the free molecular regime

With respect to composition-independent Brownian aggregation in the free molecular regime (i.e., $\rho_\mathrm{A}=\rho_\mathrm{B}$, so that $\gamma=1$), we vary systematically the relevant parameters to obtain the relation between C_2 and α, β. And it is already proved that in the free-molecular regime χ_∞/χ satisfies Eq. (3). When $\gamma=1$ and $\alpha=0.1$, C_2 is a function of χ_∞/χ_0, with different β. We use the simulation results of the fast DWMC method to fit the function $C_2=f(\chi_\infty/\chi_0)$, which is fitted to the following linear function, as shown in Fig. 5:

$$C_2=C_3\ln(\chi_\infty/\chi_0)+C_4 \tag{16}$$

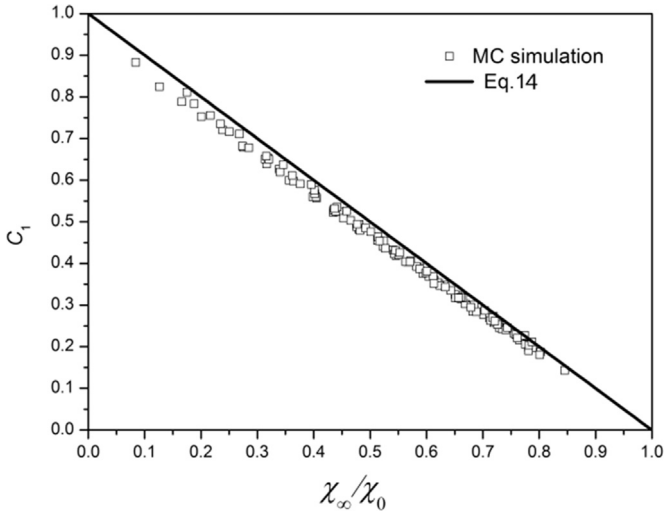

Fig. 3. χ_∞/χ_0 vs. C_1: satisfying Eq. (14) (Case 1).

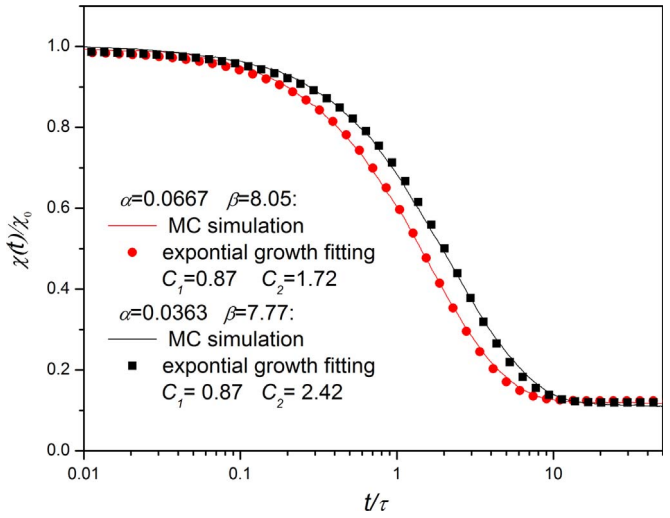

Fig. 4. χ_∞/χ_0 vs. C_2: satisfying Eq. (12) (Case 1).

We simulate 7 × 19 cases, where α=0.03, 0.067, 0.1, 0.2, 0.3, 0.43, 0.67 and ϕ are given a value among {0.05, 0.1, 0.15, 0.2, …, 0.90, 0.95}, respectively. Each one is well fitted into a linear function with an approximately equal slope C_3. Under every specified α, the values of the fitting constants C_3 are shown in Fig. 6, where it can be seen that the constants C_3 is close to 2.5.

Obviously, C_4 (the intercept presented in Fig. 6) is the function of α, $C_4 = f(\alpha)$. As shown in Fig. 8, C_4 is fitted into the following formula as:

$$C_4 = 2(\alpha + 1/\alpha)^{0.44} \tag{17}$$

To summarize, firstly we assume $\chi(t)/\chi_0$ can be fitted with an exponential decay as Eq. (12). We introduce four coefficients C_1, C_2, C_3, and C_4 altogether. Here C_2 is called exponential time constant, as the key parameter to the mixing degree, where $C_2 = f(C_3, C_4)$. Under every specified α, the values of the fitting constants C_3 are shown in Fig. 6, where the value is set as 2.5. C_4 as the function of α is shown in Fig. 7 as Eq. (17).

Therefore, $\chi(t)/\chi_0$ as a function of t can be effectively approximated as:

$$\frac{\chi(t)}{\chi_0} = \left(1 - \frac{\chi_\infty}{\chi_0}\right) \exp\left\{-t \Big/ \left[2.5 \ln\left(\frac{\chi_\infty}{\chi_0}\right) + 2(\alpha + 1/\alpha)^{0.44}\right]\right\} + \frac{\chi_\infty}{\chi_0} \tag{18}$$

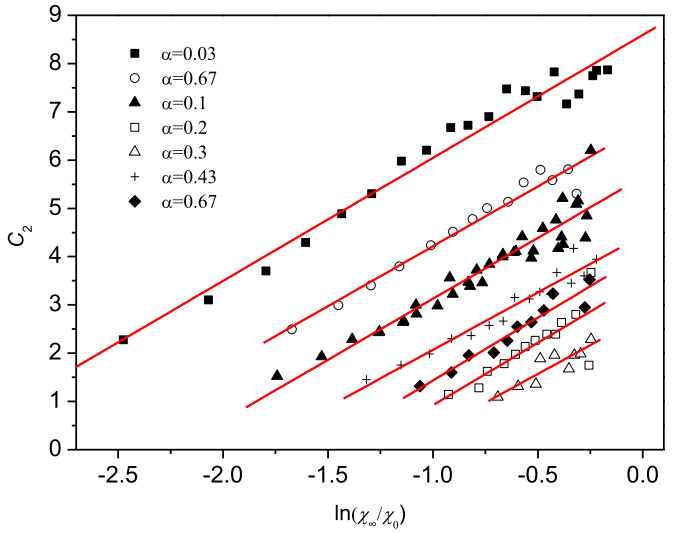

Fig. 5. C_2 as a function of χ_∞/χ_0: $\gamma=1$ and $\alpha=1$ in the free molecular regime. The linear best fit is obtained with Eq. (16). (Case 1).

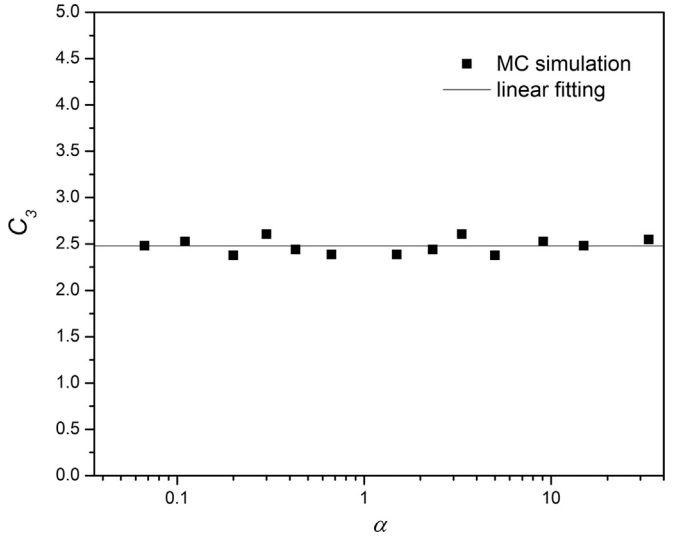

Fig. 6. Constants C_3 obtained from fitting Eq. (16) to simulation results from the MC simulations (Case 1).

If all the parameters are related to the initial state:

$$\frac{\chi(t)}{\chi_0}=\left\{1-\exp\left[-2(\phi-\phi_{\beta=1})^2\right]\right\}\exp\left\{-t/\left[-5(\phi-\phi_{\beta=1})^2+2(\alpha+1/\alpha)^{0.44}\right]\right\}$$
$$+\exp\left[-2(\phi-\phi_{\beta=1})^2\right] \tag{19}$$

so that it can be concluded that the main parameters determining $\chi(t)/\chi_0$ are the steady value of $\chi(t)/\chi_0$ overall mass fraction of component A, ϕ, and initial number ratio $\phi=\phi_{\beta=1}$, when $\gamma=1$.

In order to validate the reliability of this formula prediction, we set α at 10 as an example with varied β. Correspondingly, take $\phi=0.077$, 0.2, 0.345, 0.46, 0.58, and 0.69 as an example. Figure 8 shows the mass-normalized power density of excess component A (χ) against time made dimensionless with the characteristic aggregation time scale, τ_{coag}, which is the comparison between function prediction and the exponential decay fitting from MC simulation.

We examine whether the general exponential statistics Eq. (19) is valid for more general cases (Case 1 in Table 1) when varying both ϕ and ψ. The predictions from Eq. (19) are shown in Fig. 9. We simulate 9×9 cases, where ϕ and ψ are given a value among {0.1, 0.2, …, 0.90}, respectively. We present the simulation results and the model prediction from Eq. (18) in Fig. 9, including the standard deviations which are under 0.2 for the 81 cases (obtained by repeating each simulations 5 times). To emphasize, we ignore the cases, of which steady value χ_∞/χ_0 is over 0.9, for its slender evolution possess. In

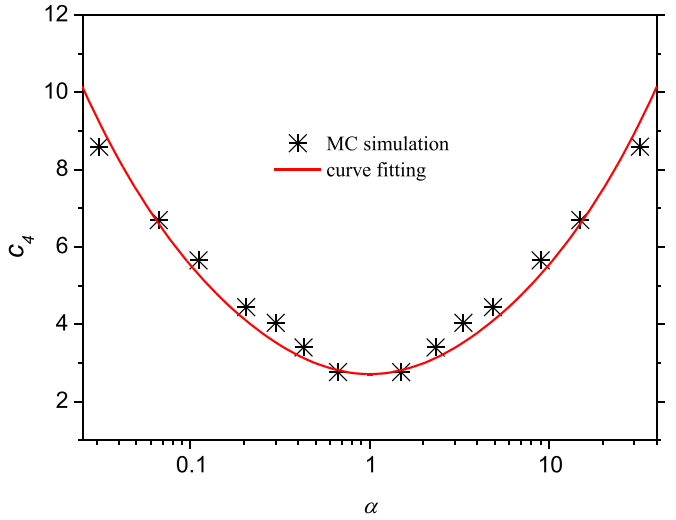

Fig. 7. C_4 as a function of α: $\gamma=1$ in the free molecular regime. The best fit is obtained with Eq. (17). (Case 1).

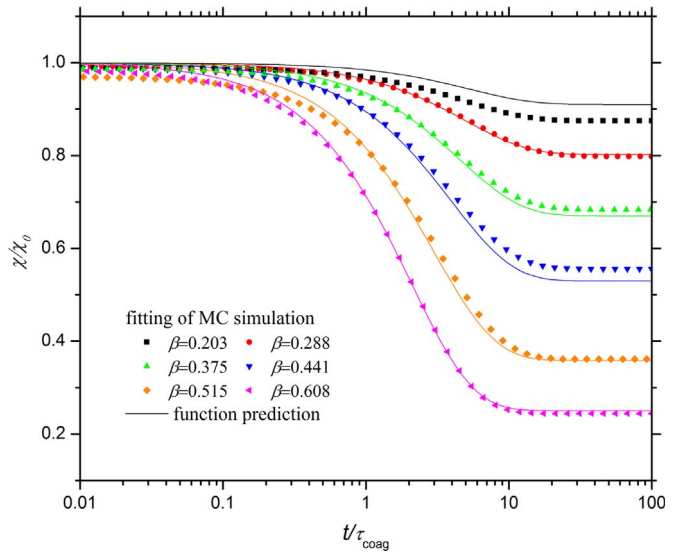

Fig. 8. Comparison between prediction and MC simulations of evolution for 6 different combinations of ϕ ($\alpha=1$, $\gamma=1$, Case 1).

view of the inherent statistical noise of MC simulations, the relation between C_2 and the initial feeding conditions is reasonably described by Eq. (18) for composition-independent aggregative mixing ($\gamma=1$).

3.4. $\chi(t)/\chi_0$ as function of α and β: in the continuum regime

In order to explore the dependency of $\chi(t)/\chi_0$ on the aggregation kernel, the same study is performed now using the kernel for the continuum regime. It is noted that this Brownian aggregation kernel is composition-independent in nature since it is related to the particle size (volume) rather than the particle mass. The fast DWMC is used to simulate 25 valid cases (Case 3 in Table 2) to explore the relation between $\chi(t)/\chi_0$ and the feeding conditions. Again, $\chi(t)/\chi_0$ satisfies the exponential function, as expressed in Eq. (21):

$$C_2 = 15\ln(\chi_\infty/\chi_0)+(\alpha+1/\alpha)^{0.75}+6 \tag{20}$$

$$\frac{\chi(t)}{\chi_0} = \left\{1-\exp\left[-(\phi-\phi_{\beta=1})^2/\sqrt{2}\right]\right\}\exp\left\{-t/\left[-10.6(\phi-\phi_{\beta=1})^2+(\alpha+1/\alpha)^{0.75}+6\right]\right\} + \exp\left[-(\phi-\phi_{\beta=1})^2/\sqrt{2}\right] \tag{21}$$

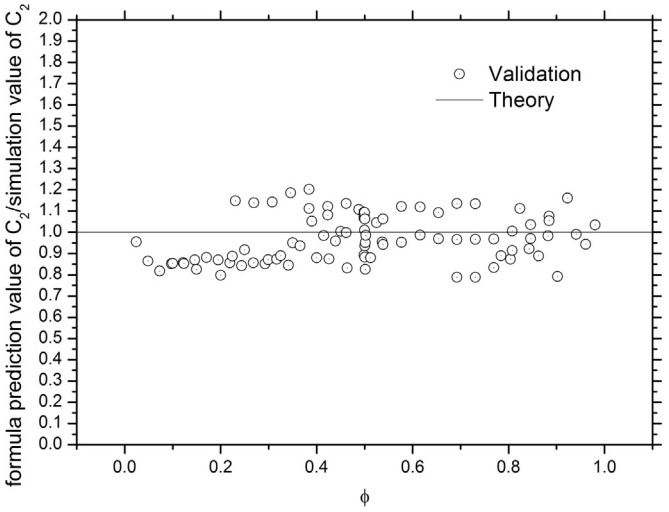

Fig. 9. Comparison between of Eq. (18) and MC simulations of C_2 for 81 different combinations of ϕ and ψ (Case 1).

3.5. $\chi(t)/\chi_0$ as function of α and β: in the transition regime A and B

Firstly, we certify the steady-state value χ_∞ which satisfies different empirical formula Eq. (3) in the transition regime A, and Eq. (4) in the transition regime B. Similarly, the fast DWMC is used to simulate 25 valid cases (Case 4 in Table 2) in the transition regime A and B respectively. In the transition regime A, by the simplified kernel, the conclusion is expressed in Eqs. (22) and (23):

$$C_2 = 2.1\ln(\chi_\infty/\chi_0)+(\alpha+1/\alpha)^{0.5}+1 \tag{22}$$

$$\frac{\chi(t)}{\chi_0} = \left\{1-\exp\left[-2(\phi-\phi_{\beta=1})^2\right]\right\}\exp\left\{-t/\left[-4.2(\phi-\phi_{\beta=1})^2+(\alpha+1/\alpha)^{0.5}+1\right]\right\} + \exp\left[-2(\phi-\phi_{\beta=1})^2\right] \tag{23}$$

In the transition regime B, with physically realistic kernel, the conclusion is expressed in Eqs. (24) and (25):

$$C_2 = 10\sqrt{2}\ln(\chi_\infty/\chi_0)+6(\alpha+1/\alpha)^{0.2} \tag{24}$$

$$\frac{\chi(t)}{\chi_0} = \left\{1-\exp\left[-(\phi-\phi_{\beta=1})^2/\sqrt{2}\right]\right\}\exp\left\{-t/\left[-10(\phi-\phi_{\beta=1})^2+6(\alpha+1/\alpha)^{0.2}\right]\right\} + \exp\left[-(\phi-\phi_{\beta=1})^2/\sqrt{2}\right] \tag{25}$$

4. Discussion

C_2 is the key parameter to control the evolution of mixing degree χ, the smaller C_2, the faster evolving. Figure 10 puts four predictor formulas together. C_2 in the free molecular is less than it in the continuum regime under the same ϕ and ψ, as particles of smaller diameter blend faster. From this point of view, the kernel in transition regime B is more accurate than A, where the value of C_2 lies between the free molecular regime and the continuum regime. Thus different kernels lead to different value of C_2, which can be used as a new benchmark for testing the kernels in multicomponent aggregation.

In addition, the time-lag for χ reaching to a steady state is equal to the time-lag for self-preserving distribution (Zhao et al., 2011). Based on Eq. (12), we take the free molecular regime as an example. When $\chi(t)/\chi_0=0.99\chi_\infty/\chi_0$, the steady-state is reached. And the time-lag can be calculated as:

$$t_{\text{lag}} = \left[\ln\left(\frac{0.01\chi_\infty}{\chi_0}\right)\right]\left[2.5\ln\left(\frac{\chi_\infty}{\chi_0}\right)+2(\alpha+1/\alpha)^{0.44}\right] \tag{26}$$

where the unit of time is characteristic aggregation time scale τ_{coag}, which is defined as $1/(2\bar{K}_0N_0)$.

Also the compositional distribution is able to be calculated through the predict formula in the feeding condition. Since all the above fitting formula is obtained under the condition of $g=1$, here we further investigate the dependence of γ. Using case 2, the synthesis of FePt nanoparticles is taken as an example (Lin et al., 2009). We use Eq. (19) to calculate dimensionless mixing degree and substitute it into Eq. (2) for composition distribution. The result is well matched as Fig. 11 show.

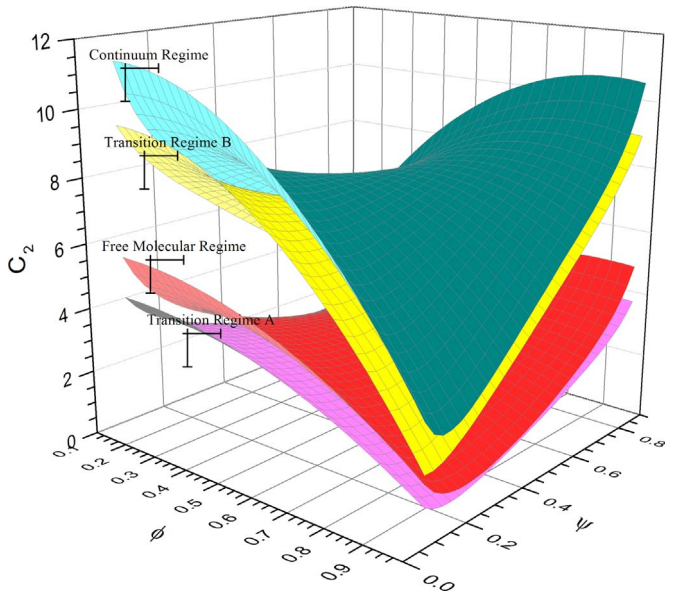

Fig. 10. C_2 as a function of ϕ and ψ in different regimes ($\gamma=1$).

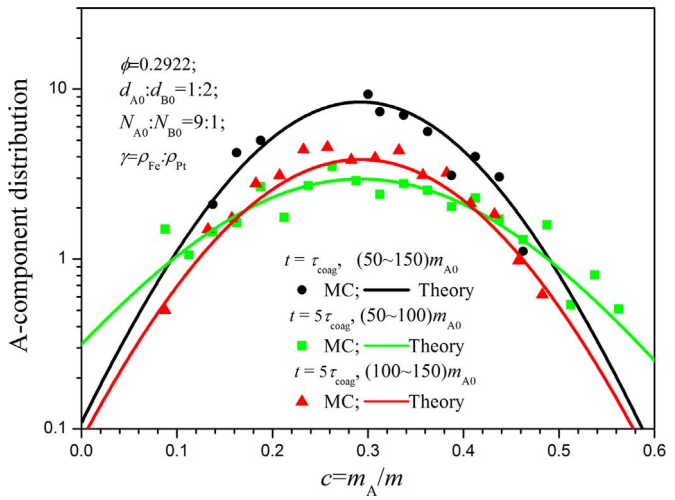

Fig. 11. Compositional distributions within selected intervals: comparison between the formula predictions and the PBMC simulations (Case 2).

Thus Eq. (19) is valuable in the free molecular regime when $\gamma=\rho_{Fe}/\rho_{Pt}$. Zhao & Kruis (2014) certified Eq. (3) seemed to be able to predict χ_∞/χ_0 reasonably, but with a decreasing reliability. However when we change the γ value, or take other regimes with $\gamma \neq 1$, the reliability of the prediction function varies, for both steady-state value and process value. There requires further study to determine a more accurate formula on various γ.

5. Conclusions

The feeding condition is of vital important for two-component aggregative mixing, where the whole evolution process is able to be predicted based on the initial mixture state of the components, e.g. the ratio of the particle volume of the two components at the start of the aggregation process. With respect to two-component aggregative mixing due to Brownian coagulation with initially bidisperse distributions, simulations demonstrate the changing over time of mass-normalized power density of excess component A. $\chi(t)$ can be characterized by an exponential function with a known steady-state value of χ (χ_∞). This exponential-type function is determined by the number ratio and the particle diameter ration between two components. We add the fitting function with the overall mass fraction of component A (Φ) and steady-state mixing degree (χ_∞) to simplify the formation. A good estimation of $\chi(t)$ is given by the exponential function in Eq. (19) for Brownian

aggregation in the free molecular regime, Eq. (21) in the continuum regime, and Eqs. (23) and (25) in the transition regime for different kernel. So the time to reach the steady-state is known and the probability density $g(m_A|m)$ is able to achieve in advance, e.g., the mixing degree during two-component aggregation process. The proposed functions would be conducive to control the whole experimental investigation evolution of the composition of sufficiently large numbers of individual particles formed by bicomponent aggregation.

Acknowledgments

This study was supported with funds from the National Natural Science Foundation of China (51276077, 51390494 and 51522603).

References

Barrasso, D., & Ramachandran, R. (2012). A comparison of model order reduction techniques for a four-dimensional population balance model describing multi-component wet granulation processes. *Chemical Engineering Science*, *80*, 380–392.
Friedlander, S. K., & Smoke, D. (2000). *Haze: fundamentals of aerosol dynamics* (p. 308)*New York*: *Oxford University Press*308.
Hofmann, S., & Raisch, J. (2013). Solutions to inversion problems in preferential crystallization of enantiomers—Part II: batch crystallization in two coupled vessels. *Chemical Engineering Science*, *88*, 48–68.
Hosseini, A., Bouaswaig, A. E., & Engell, S. (2013). Novel approaches to improve the particle size distribution prediction of a classical emulsion polymerization model. *Chemical Engineering Science*, *88*, 108–120.
Iveson, S. M. (2002). Limitations of one-dimensional population balance models of wet granulation processes. *Powder Technology*, *124*(3), 219–229.
Jacobson, M. Z. (2005). *Fundamentals of atmospheric modeling*. United Kingdom: Cambridge university press.
Kazakov, A., & Frenklach, M. (1998). Dynamic modeling of soot particle coagulation and aggregation: implementation with the method of moments and application to high-pressure laminar premixed flames. *Combustion and Flame*, *114*(3), 484–501.
Krapivsky, P., & Ben-Naim, E. (1996). Aggregation with multiple conservation laws. *Physical Review E*, *53*(1), 291.
Kuang, C., McMurry, P., & McCormick, A. (2009). Determination of cloud condensation nuclei production from measured new particle formation events. *Geophysical Research Letters*, *36*(9).
Lee, K., Kim, T., Rajniak, P., & Matsoukas, T. (2008). Compositional distributions in multicomponent aggregation. *Chemical Engineering Science*, *63*(5), 1293–1303.
Lin, J., Loh, L., Lee, P., Tan, T., Springham, S., & Rawat, R. (2009). Effects of target–substrate geometry and ambient gas pressure on FePt nanoparticles synthesized by pulsed laser deposition. *Applied Surface Science*, *255*(8), 4372–4377.
Liu, Y., Jiang, Y., Zhang, X., Wang, Y., Zhang, Y., Liu, H., & Yan, Y. (2014). Structural and magnetic properties of the ordered $FePt_3$, FePt and Fe_3Pt nanoparticles. *Journal of Solid State Chemistry*, *209*, 69–73.
Lushnikov, A. (1976). Evolution of coagulating systems: III. Coagulating mixtures. *Journal of Colloid and Interface Science*, *54*(1), 94–101.
Marshall, C. L., Rajniak, P., & Matsoukas, T. (2011). Numerical simulations of two-component granulation: comparison of three methods. *Chemical Engineering Research and Design*, *89*(5), 545–552.
Matsoukas, T., Kim, T., & Lee, K. (2009). Bicomponent aggregation with composition-dependent rates and the approach to well-mixed state. *Chemical Engineering Science*, *64*(4), 787–799.
Matsoukas, T., Lee, K., & Kim, T. (2006). Mixing of components in two-component aggregation. *AIChE Journal*, *52*(9), 3088–3099.
Patterson, R. I., Singh, J., Balthasar, M., Kraft, M., & Wagner, W. (2006). Extending stochastic soot simulation to higher pressures. *Combustion and Flame*, *145*(3), 638–642.
Vigil, R. D., & Ziff, R. M. (1998). On the scaling theory of two-component aggregation. *Chemical Engineering Science*, *53*(9), 1725–1729.
Wei, J. (2014). A majorant kernel-based Monte Carlo method for particle population balance modeling. *Aerosol and Air Quality Research*, *14*(3), 623–631.
Xu, Z., Zhao, H., & Zheng, C. (2014). Fast Monte Carlo simulation for particle coagulation in population balance. *Journal of Aerosol Science*, *74*, 11–25.
Xu, Z., Zhao, H., & Zheng, C. (2015). Accelerating population balance-Monte Carlo simulation for coagulation dynamics from the Markov jump model, stochastic algorithm and GPU parallel computing. *Journal of Computational Physics*, *281*, 844–863.
Zeng, P., Zhou, T., & Yang, J. (2008). Behavior of mixtures of nano-particles in magnetically assisted fluidized bed. *Chemical Engineering and Processing: Process Intensification*, *47*(1), 101–108.
Zhao, H., & Kruis, F.Einar (2014). Dependence of steady-state compositional mixing degree on feeding conditions in two-component aggregation. *Industrial Engineering Chemistry Research*, *53*(14), 6047–6055.
Zhao, H., Kruis, F. E., & Zheng, C. (2010). A differentially weighted Monte Carlo method for two-component coagulation. *Journal of Computational Physics*, *229*(19), 6931–6945.
Zhao, H., Kruis, F. E., & Zheng, C. (2011). Monte Carlo simulation for aggregative mixing of nanoparticles in two-component systems. *Industrial Engineering Chemistry Research*, *50*(18), 10652–10664.
Zhao, H., & Zheng, C. (2011). Two-component Brownian coagulation: Monte Carlo simulation and process characterization. *Particuology*, *9*(4), 414–423.
Zhao, H., & Zheng, C. (2013). A population balance-Monte Carlo method for particle coagulation in spatially inhomogeneous systems. *Computers Fluids*, *71*, 196–207.